

Highlights from the COMPASS experiment

G. K. Mallot^{1,1)}

On behalf of the COMPASS Collaboration
1 (CERN, PH Department, 1211 Geneva 23, Switzerland)

Abstract The COMPASS experiment at CERN is studying the nucleon spin structure with a 160 GeV polarized muon beam and polarized targets as well as hadron structure with 190 GeV pion, kaon and proton beams. The Paper gives an overview of the results for the helicity and transverse spin structure of the nucleon. A first result from the spectroscopy experiments, the observation of a resonance with exotic $J^{PC} = 1^{-+}$ quantum numbers at 1660 MeV is also presented. The Paper ends with an outlook to future measurements.

Key words nucleon structure, spin, deep inelastic scattering, hadron spectroscopy, exotic mesons

PACS 13.60.Le, 13.85.Hd, 14.20.Dh, 14.40.Be, 14.40.Rt

1 Introduction

The COMPASS fixed-target experiment at the CERN Super-Proton-Synchrotron (SPS) unites about 240 physicists in the study of the nucleon spin structure and of the spectroscopy of hadrons. The measurements at the SPS M2 beam line started 2002 and were performed using muons of 160 GeV and pions and protons of 190 GeV, respectively. The incoming and outgoing particles are analyzed in a common, 50 m long spectrometer^[1] with two dipole magnets and charged particle tracking. Particle identification is performed by a RICH detector with pion/kaon separation from 9–50 GeV/ c and two hadronic calorimeters. Photons are detected by two electromagnetic calorimeters.

The spin structure measurements require polarized beam and targets. The muon beam is naturally polarized to about 80% due to the weak pion decay. The large polarized target comprises a magnet system with a 2.5 T solenoid and a 0.5 T dipole, a dilution refrigerator, a microwave system for dynamic nuclear polarization and NMR coils to measure the polarization. The target material is contained in two or three cells with a total length of 1.2 m and polarized oppositely in adjacent cells. Typical polarizations were 85% for the proton material (NH_3) and 50% for the deuteron material (^6LiD). The dilution factor amounts to about 0.18 and 0.4 for the two materials, respectively. With 5×10^7 muons/s and a duty

factor of the SPS of 20–33% the nominal luminosity is in the order of $5 \times 10^{32} \text{ cm}^{-2}\text{s}^{-1}$ (not accounting for polarization). Data with a deuteron target were taken from 2002–2006 and with a proton target in 2007. Following a short pilot run in 2004, the years 2008 and 2009 were dedicated to spectroscopy measurements with hadron beams.

2 Helicity structure

The cross-section for deep-inelastic scattering (DIS) of leptons from nucleons factorizes into a hard part, calculable in perturbative QCD, and a non-perturbative part containing the information on internal structure of the nucleon. The latter is parameterized in terms of parton distribution functions (PDF) for quarks and gluons as a function of the momentum fraction x carried by the parton. The role of the various quark flavours can be investigated by combining proton and neutron (deuteron) data. Another tool providing such information is semi-inclusive DIS (SIDIS) in which a produced hadron is observed in addition to the scattered lepton. In particular, when this hadron carries a large fraction z of the total transferred energy, the originally struck quark flavour is reflected in the hadron type. The fragmentation of a quark q into a hadron h is described by the fragmentation function (FF) $D_q^h(z, Q^2)$. A fragmentation is favoured if the original quark is contained in the final hadron, e.g. $u \rightarrow \pi^+$.

Received 19 January 2010

1) E-mail: gerhard.mallot@cern.ch

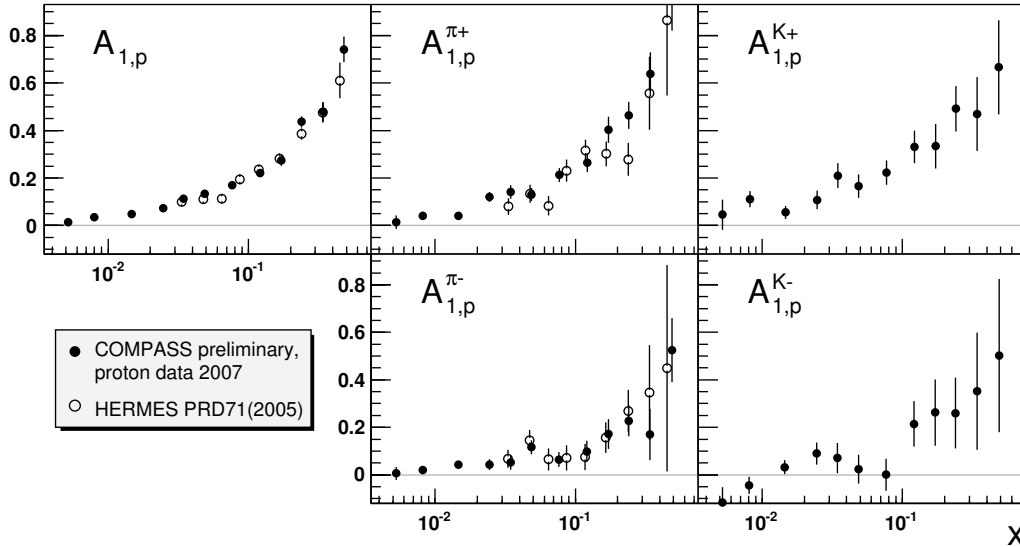


Fig. 1. Inclusive and semi-inclusive virtual-photon asymmetries of the proton A_1 and A_1^h for identified pions and kaons as function of x . For comparison the results from HERMES^[2] are shown where available. The error bars represent the statistical uncertainties.

The virtual-photon–nucleon cross-section asymmetry A_1 for SIDIS is given by

$$A_1(x, Q^2, z) = \frac{\sum_q e_q^2 \Delta q(x, Q^2) D_q^h(z, Q^2)}{\sum_q e_q^2 q(x, Q^2) D_q^h(z, Q^2)}, \quad (1)$$

where $q = q^+ + q^-$ and $\Delta q = q^+ - q^-$ are the spin-averaged and the helicity quark distributions, e_q are the quark charges and $-Q^2$ is the 4-momentum transfer. The COMPASS proton data for the inclusive asymmetry ($D \equiv 1$) and the semi-inclusive asymmetries are shown in Fig. 1 integrated over $0.2 < z < 0.85$. Apart from the data for positive and negative pions, proton asymmetries for identified kaons were measured, the latter for the first time. The asymmetries for the deuteron were published earlier.^[3]

Below $x \simeq 0.02$ previously only the data from the Spin Muon Collaboration were available. The precision of the inclusive asymmetries for the proton and the deuteron in this region were improved by the new measurements by a factor 2.5 and 6, respectively. The spin-dependent structure function g_1 is related to the asymmetry by $g_1 = A_1 F_1$. From our deuteron data we determined^[4] the flavour-singlet axial matrix element a_0 , which in the $\overline{\text{MS}}$ scheme is identical to the fraction of the nucleon spin carried by the quark spins $\Delta\Sigma$, and the first moment of the strange sea for $Q^2 \rightarrow \infty$ as

$$\begin{aligned} a_0 &= 0.33 \pm 0.03 (\text{stat.}) \pm 0.05 (\text{syst.}) \\ \Delta s + \Delta \bar{s} &= -0.08 \pm 0.01 (\text{stat.}) \pm 0.02 (\text{syst.}). \end{aligned} \quad (2)$$

As visible in Fig. 2 the new precise proton data lie in

the previously poorly known high- Q^2 /small- x region and thus will have a considerable impact on future QCD analyzes of the world g_1 data.

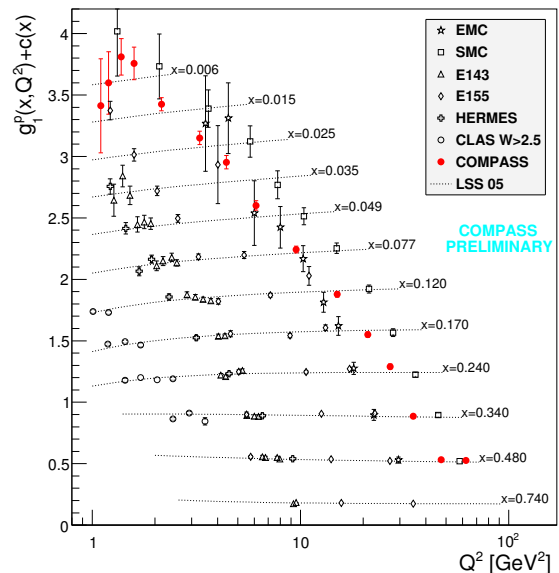


Fig. 2. The spin-dependent structure function g_1 of the proton as function of Q^2 for fixed values of x . For readability the data points belonging to different x bins were displaced vertically.

Combining the proton data with the deuteron data will lead to an improved test of the fundamental Bjorken sum rule for first moment of the non-singlet structure function $g_1^{\text{NS}} = g_1^p - g_1^n$ shown in Fig. 3.

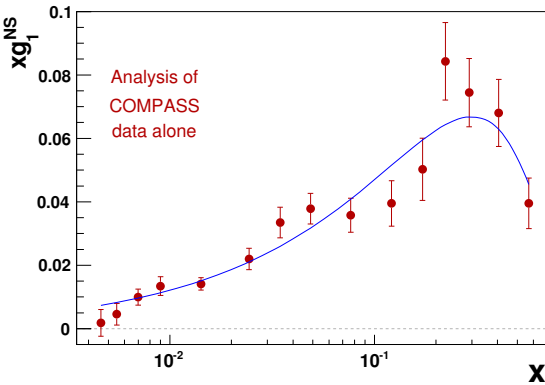


Fig. 3. The non-singlet structure function g_1^{NS} as function of x at $Q^2 = 3$ (GeV/c)². The curve represents a NLO QCD fit to the COMPASS data.

From the inclusive and semi-inclusive asymmetries we determined the spin-dependent PDFs Δu , Δd , $\Delta \bar{u}$, $\Delta \bar{d}$ and Δs as well as the flavour asymmetry of the light quark sea $\Delta \bar{u} - \Delta \bar{d}$. In this leading-order (LO) analysis a symmetric strange sea $\Delta s = \Delta \bar{s}$ was assumed as in our previous analysis of the deuteron data.^[3] In LO the semi-inclusive asymmetries are given by

$$A^h(x) = \sum_q \mathcal{P}_q(x) \frac{\Delta q(x)}{q(x)}, \quad \text{where}$$

$$\mathcal{P}_q^h(x) = \frac{e_q^2 q(x) D_q^h}{\sum_{q'} e_{q'}^2 q'(x) D_{q'}^h} \quad (3)$$

represents the contribution of quark flavour q to the production of hadron h . Such an analysis crucially depends on the fragmentation functions D . Several sets of FF were used. They yield similar purities \mathcal{P} for pions but differ e.g. for the fraction of K^- coming from u versus s quarks and of K^+ originating from \bar{u} versus \bar{s} quarks. For our analysis we chose the DSS FF^[5], which are best adapted to the COMPASS kinematics. The resulting PDFs are shown in Fig. 4. The new data agree well with the less precise HERMES data and extend down to $x = 0.005$. Our data do not show negative values of the strange sea at around $x = 0.2$ like the DNS fit^[6]. However, there is possibly a hint of negative values at smaller x . Inclusive data in conjunction with SU(3) flavour symmetry require a negative first moment for Δs . Again the new data will impact the QCD fits to the world data, e.g. the DSSV fits.^[7]

The flavour asymmetry of the unpolarized light quark sea $\bar{u} - \bar{d} < 0$ is an established fact since long. A non-vanishing asymmetry is also expected by models for the polarized case $\Delta \bar{u} - \Delta \bar{d}$. We find a small

positive asymmetry as shown in Fig. 5. The integral over the measured range $0.004 < x < 0.3$ is 0.052 ± 0.035 (stat.) ± 0.013 (syst.).

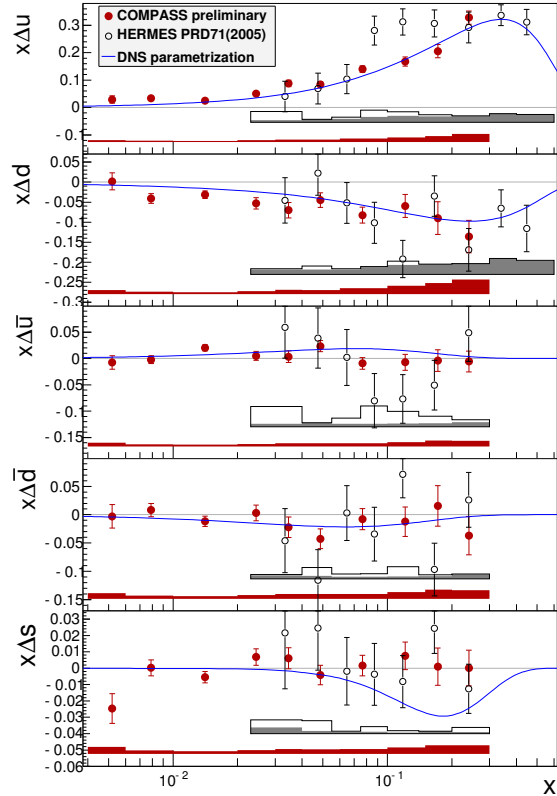


Fig. 4. The quark helicity distributions evaluated at common value of $Q^2 = 3$ GeV^2 as a function of x . The bands represent the systematic uncertainties. For comparison also the HERMES data^[2] and the LO DNS parametrization^[6] is shown.

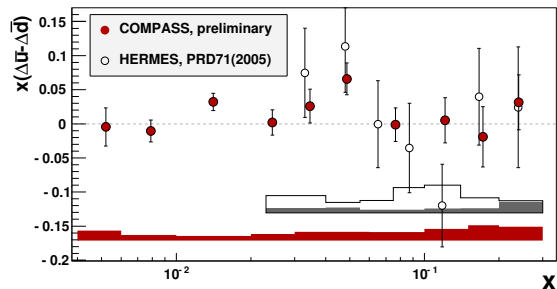


Fig. 5. Flavour asymmetry in the helicity densities of the light sea, $\Delta \bar{u} - \Delta \bar{d}$ as function of x at $Q^2 = 3$ GeV^2 .

3 Gluon polarization

Following the finding by the EMC that the contribution of the quark spins $\Delta \Sigma$ to the nucleon spin is small, it was suggested that a very large gluon polarization masks the contribution of the quark spins via

the axial anomaly. Such a gluon polarization would have to be compensated by orbital angular momentum in order to conserve the nucleon spin of 1/2, which is made up by the quark and gluon spins and orbital angular momentum

$$\frac{1}{2} = \frac{1}{2} \Delta \Sigma + \Delta G + L_z. \quad (4)$$

In inclusive DIS the gluon polarization can only be accessed via the scaling violations of structure functions. However, the Q^2 and x range of the experimental data is insufficient for a precise determination. The photon–gluon fusion (PGF) process, in which a quark–antiquark pair is produced, is a direct probe for the gluon distribution. The observed cross-section asymmetry for the production of hadrons originating from the quark–antiquark pair is proportional to the gluon polarization. The average analyzing power of the process and the contribution from other processes need to be determined by Monte Carlo simulations. In COMPASS we studied three processes: the production of light hadron pairs with large- p_T and 4-momentum transfers of $Q^2 > 1 \text{ GeV}^2$ and of $Q^2 < 1 \text{ GeV}^2$, and open charm production mainly by quasi-real photons. For the former processes the hard scale is established by the transverse momentum p_T of the hadrons while the charm mass sets the scale in the latter process. Because charmed D mesons essentially originate entirely from PGF this is a very clean process. However, due to the small production cross-section and the branching ratio of about 4% for the most accessible decay channel $D \rightarrow \pi K$ this process is difficult to measure. The high combinatorial background in this channel is considerably suppressed when tagging D mesons originating from $D^* \rightarrow D \pi_s$ via detection of the slow pion π_s . Up to now all PGF analyzes were performed in LO; NLO calculations are ongoing.

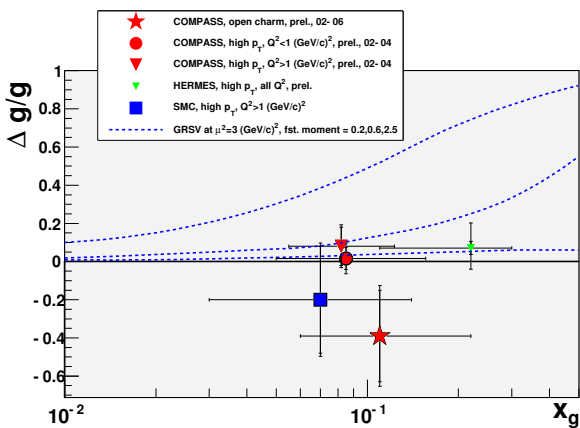


Fig. 6. Gluon polarization from LO PGF analyzes shown at the average x of the gluon. Also shown are the parameterizations by GRSV [8].

The results summarized in Fig. 6 prefer small values of the gluon polarization. The curves corresponds to $\Delta G = 2.5, 0.6$ and 0.2 from top to bottom. Values of the order of 2.5 or more for the first moment ΔG as suggested in the wake of the EMC discovery are now very unlikely. However, a sizable contribution of the gluon spins to the nucleon spin cannot be excluded at the present stage.

4 Transverse spin structure

For a complete collinear description of the nucleon at the twist-2 level another PDF is required. Transversity, denoted by h_1 or $\Delta_T q$, describes the distribution of transversely polarized partons in a transversely polarized nucleon. In the non-relativistic case h_1 is equal to g_1 . Being chirally odd, this PDF cannot be observed in inclusive DIS because chirality is conserved at the vertex. However, in SIDIS the additional hadron allows the restoration of chirality by combining the chirally odd PDF with a chirally odd FF. Best known is the Collins FF $\Delta_T^0 D_q^h$. It causes an azimuthal single-spin cross-section asymmetry $\Delta\sigma/\sigma \propto A_{Coll} \sin\Phi_C$, where $\Phi_C = \phi_h - \phi_S - \pi$ is given by the azimuth angles of the hadron and of the nucleon spin with respect to the scattering plane. The Collins asymmetry can then be expressed as

$$A_{Coll} = \frac{\sum_q e_q^2 \Delta_T q(x) \Delta_T^0 D_q^h(z, p_T)}{\sum_q e_q^2 q(x) D_q^h(z, p_T)}. \quad (5)$$

A clear signal is visible in our proton asymmetries shown in Fig. 7. In the region of overlap the results are in good agreement with those from HERMES. For the deuteron^[9] the observed asymmetries are compatible with zero, implying that the transversity PDFs of the up and down quarks have opposite signs. This is also reflected in the sign change of the Collins asymmetries going from positive to negative hadrons.

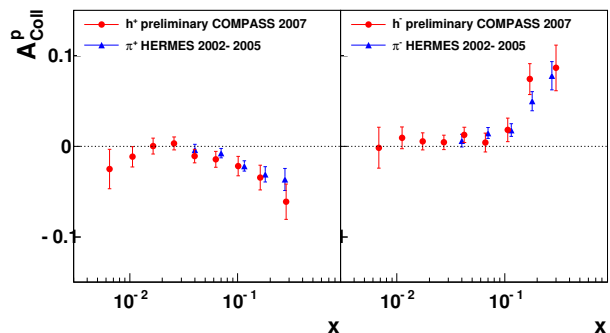


Fig. 7. The Collins asymmetries for the proton as function of x for positive (left) and negative hadrons (right). For comparison also results from HERMES are shown.

The transversity distribution can also be coupled to the chirally odd interference FF H_1^{\langle} , which describes fragmentation into a hadron pair. This generates an azimuthal $\sin \Phi_{RS}$ asymmetry, where $\Phi_{RS} = \phi_R + \phi_S - \pi$ and ϕ_R is the azimuthal angle between the scattering plane and the plane defined by the hadron pair. The observed large asymmetries A_{RS} for the proton are shown in Fig. 8, the asymmetry is also presented as a function of the invariant mass M_{inv} . The change in A_{RS} predicted by some models in the ρ mass region is not observed.

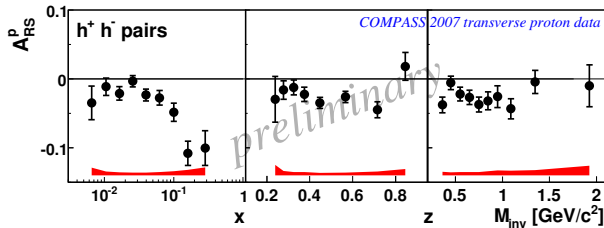


Fig. 8. Two-hadron asymmetries for the proton as function of x , z and M_{inv} .

Taking into account the intrinsic transverse momentum k_T of quarks, the total number of structure functions increases from three to eight of which only f_1 , g_1 , and h_1 survive upon integration over k_T . Of particular interest is the Sivers function f_{1T}^{\perp} describing unpolarized quarks in a transversely polarized nucleon. This function coupled to the standard unpolarized FF gives rise to an azimuthal $\sin \Phi_S$ asymmetry, where $\Phi_S = \phi_h - \phi_S$. For the deuteron we observe small asymmetries compatible with zero.^[9] The proton asymmetries are within the statistical precision compatible with zero (Fig. 9) and do not exhibit the strongly positive trend with x seen in the HERMES data for positive hadrons. For negative hadrons both HERMES and COMPASS find zero asymmetries.

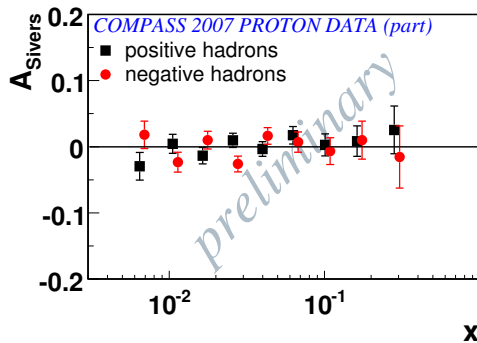


Fig. 9. Sivers asymmetry for the proton as function of x for positive (squares) and negative hadrons (spheres).

5 Spin transfer to Λ s

Another subject studied at COMPASS is the longitudinal spin transfer D_{LL} from the virtual photon to Λ s and $\bar{\Lambda}$ s.^[10] A significantly positive D_{LL} is found for $\bar{\Lambda}$ s with a trend to increase with the longitudinal momentum fraction x_F , while for Λ s the spin transfer is compatible with zero (Fig. 10). Models predict that the spin transfer to Λ ($\bar{\Lambda}$) strongly depends on the (anti-)strange quark distribution.^[11]

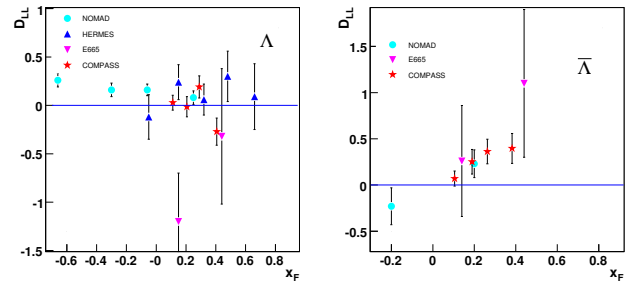


Fig. 10. The longitudinal spin transfer D_{LL} for Λ s (left) and $\bar{\Lambda}$ s (right) as function of x_F . For comparison data from NOMAD, E665 and HERMES are also shown.

6 Physics with hadron beams

In 2004 COMPASS had a short pilot run with a 190 GeV pion beam for the spectroscopy program. In 2008 and 2009 a huge data set with pion, kaon and proton beams was taken and first results were presented on this conference.^[12] Here we present a partial-wave analysis of the 2004 data for the 3π final state in the reaction $\pi^- + \text{Pb} \rightarrow \pi^- \pi^- \pi^+ \text{Pb}$.^[13] In three days an event sample was recorded with 420'000 events in the range $0.1 \text{ GeV}^2 < t' < 1 \text{ GeV}^2$, where $t' = t - t_{\min}$ and t is the momentum transfer to the 3π system. The invariant mass of this system is shown in Fig. 11. The well-known resonances $a_1(1260)$, $a_2(1320)$ and $\pi_2(1670)$ are clearly visible.

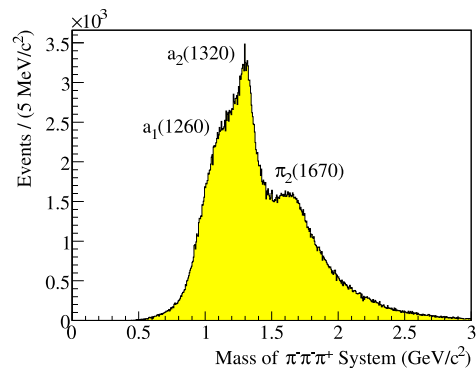


Fig. 11. Invariant mass of the 3π system for $0.1 \text{ GeV}^2 < t' < 1 \text{ GeV}^2$.

A partial-wave analysis was performed in two steps after applying moderate acceptance corrections. First, a mass-independent fit of the amplitudes of 42 waves was performed in each of the 40 MeV mass bin. In a second step, the resulting mass spectra for the various waves were fitted by relativistic Breit–Wigner functions. Here only a subset containing the six major waves was used. In addition to the major $q\bar{q}$ resonances visible in Fig. 11, we find a resonance with exotic quantum numbers $J^{PC} = 1^{-+}$ at 1660 MeV decaying into $\rho\pi$ (Fig. 12).

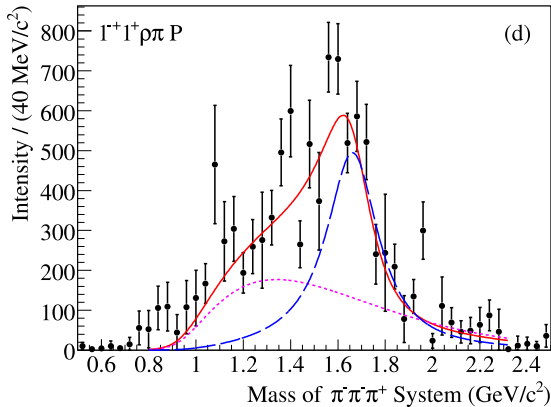


Fig. 12. Intensity of the exotic wave $1^{-+}1^+\rho\pi P$. In addition to the Breit–Wigner contribution (dashed) a non-resonant background (dotted) is fitted, maybe caused by a Deck-like effect. The solid line is the total fitted intensity.

The resonant nature of this wave is demonstrated by its phase motion with respect to the $a_1(1260)$ and the $\pi_2(1670)$ in the $J^{PC}M^\epsilon[\text{isobar}]L = 1^{++}0^+\rho\pi S$ and $2^{-+}0^+f_2\pi S$ channel, respectively (Fig. 13).

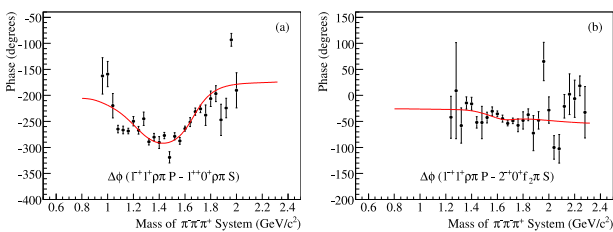


Fig. 13. Invariant mass of the 3π system for $0.1 \text{ GeV}^2 < t' < 1 \text{ GeV}^2$.

For the a_1 a clear phase motion is visible, because it is not resonating at this mass anymore. On the

contrary the phase motion of the close-by π_2 is similar to that of the exotic and thus the relative phase motion is small.

The observed resonance is consistent with the highly debated $\pi_1(1600)$.

7 Outlook

The next steps in the COMPASS program are to complete the spin structure studies on the proton both with longitudinal and transverse polarization. The measurements will restart with transverse polarization in 2010. In the hadron physics programme we plan measurements of the pion and maybe the kaon polarisability as well as further data taking for the spectroscopy investigations. A proposal is in preparation aiming at measurements of generalized parton distributions focussing on deep virtual Compton scattering and at a further study of transversity and transverse-momentum dependent structure function in the Drell–Yan process using a pion beam impinging on a transversely polarized proton target.

References

- 1 P. Abbon *et al.* [COMPASS Collaboration], Nucl. Instrum. Meth. A **577** (2007) 455.
- 2 A. Airapetian *et al.* [HERMES Collaboration], Phys. Rev. D **71** (2005) 012003.
- 3 M. Alekseev *et al.* [COMPASS Collaboration], Phys. Lett. B **680** (2009) 217.
- 4 E. S. Ageev *et al.* [Compass Collaboration], Phys. Lett. B **647** (2007) 330.
- 5 D. de Florian, R. Sassot, M. Stratmann, Phys. Rev. D **75** (2007) 114010; D **76** (2007) 074033.
- 6 D. de Florian, G. A. Navarro, R. Sassot, Phys. Rev. D **71** (2005) 094018.
- 7 D. de Florian, R. Sassot, M. Stratmann and W. Vogelsang, Phys. Rev. D **80** (2009) 034030.
- 8 M. Glück, E. Reya, M. Stratmann and W. Vogelsang, Phys. Rev. D **63** (2001) 094005.
- 9 M. Alekseev *et al.* [COMPASS Collaboration], Phys. Lett. B **673** (2009) 127
- 10 M. Alekseev *et al.* [COMPASS Collaboration], Eur. Phys. J. C **64** (2009) 171
- 11 J. R. Ellis, A. Kotzinian, D. Naumov and M. Sapozhnikov, Eur. Phys. J. C **52** (2007) 283.
- 12 I. Uman, these proceedings.
- 13 M. Alekseev *et al.*, [COMPASS Collaboration], arXiv:0910.5842 [hep-ex].